Scanning Microscopy

Volume 7 | Number 1 Article 31

1-20-1993

Scanning Electron Microscopy of Styrene-Methylethylketone Casts of the Airway and the Arterial System of the Lung

Teruyuki Hojo
University of Occupational and Environmental Health, Kitakyushu

Scanning Microscopy, Vol. 7, No. 1, 1993 (Pages 287-293)
Scanning Microscopy International, Chicago (AMF O'Hare), IL 60666 USA

0891-7035/93$5.00+.00

SCANNING ELECTRON MICROSCOPY OF STYRENE-METHYLETHYLKETONE CASTS OF THE AIRWAY AND THE ARTERIAL SYSTEM OF THE LUNG

Teruyuki Hojo

Department of Anatomy and Anthropology
University of Occupational and Environmental Health, School of Medicine,
Kitakyushu City 807, Japan

Telephone: (81) 93 691-7232; FAX:(81) 93 691-8544

(Received for publication July 22, 1992, and in revised form January 20, 1993)

Abstract

The method of making casts of airways and the pulmonary arterial system using a styrene polymer resin is described. A human and a dog were used as models. The viscosity of this resin ranges between 40 and 60 dPa/s at 24°C. The elastic rubber tube used for resin injection allows a constant perfusion pressure, i.e., 44 mm Hg and 110 mm Hg for airway and vascular filling, respectively. The casts obtained using this method are suitable both for macro- and microscopic analysis. Shrinkage during polymerization is minimal. Moreover, a preceding lavage is not necessary. Scanning electron microscopy (SEM) of cast lungs showed the endothelial cell nuclei imprints on vessels. Computer assisted analysis of alveolar capillary interspaces showed that these holes are larger than those described in normal rats. The diameter of alveolar capillaries in dogs is almost the same as in the normal rat lung. When casting the airways, alveolar cells and/or materials inhaled might be preserved and observed in SEM.

Key Words: Scanning electron microscopy, corrosion casting, styrene-methylethylketone, lung, bronchioles, alveoli, capillaries, human, dog.

Introduction

In the past, I have made anatomical studies in the lung using macrocorrosion casts of large mammals, e.g., humans, dogs, seals, and otaries to observe the three-dimensional branching pattern of airways and blood vessels (Hojo, 1974; 1975a; 1975b; 1980; Hojo *et al.*, 1989). The resin I have used was prepared by dissolving a styrene polymer in methylethylketone. Latex or methylmethacrylate have been reported to be used for similar studies (Aharinejad *et al.*, 1991a; 1991b; Charan *et al.*, 1984; Dilly, 1986; Guntheroth *et al.*, 1982; Hodde, *et al.*,1990; Hossler and West, 1988; Kendall and Eissmann, 1980; Koike *et al.*, 1986; Lametschwandtner *et al.*, 1976; 1990; Ohtani, 1980; Piasecki, 1974; Rodriguez *et al.*, 1987; Schlesinger and McFadden, 1981; Schraufnagel, 1987; 1990; Schraufnagel *et al.*, 1986; Schraufnagel and Patel, 1990; Schraufnagel and Schmid, 1988). While Hodde *et al.* (1990) used a Harvard infusion pump, most authors did not perfuse the resin at a constant pressure. This may be because instruments to deliver a constant pressure are cumbersome and expensive. In this paper, I describe a method of making lung casts using a screw syringe attached to a flexible rubber tubing that provides constant pressure in a simple manner. Using this method, I was able to compare the dog and human lung microvasculature as well as airway microanatomy.

Materials and Methods

Styrene polymer was obtained from Koso Kagaku Co. (Tokyo) and dissolved in methylethylketone (in 2:3 weight ratio) in a closed flask at room temperature. After about 2 hours, the mixture completely dissolves and can be poured into a special 314 ml brass screw syringe made by Kenmeisha Co. (Fukuoka City; Figure 1). The viscosity of this resin ranges between 40 and 60 dPa/s at 24°C. The end of the syringe (3 mm inner and 5 mm outer diameter) was connected to a 15 cm long rubber tube (8 mm inner and 11 mm outer diameter). This was connected to a plastic cannula of 6 mm inner and 10 mm outer diameter, with the end of the cannula introduced into a vessel or trachea. The cannula was ligated into

place by a linen thread. The elasticity of this flexible rubber tube imparts a constant pressure as the plunger of the syringe is advanced.

The trachea of a 55-year-old man, who died of heart failure, was cannulated (inner diameter 8 mm) and 700 ml of the resin was injected through the cannula. The lung had been fixed with 10% formalin. The pressure required to fill the airways was about 44 mm Hg, the pressure to fill the vascular space was about 110 mm Hg. The injection pressure, measured at the connection of the rubber tube with the syringe, was kept as constant as possible. To cast the airway of the 12-kg dog, about 500 ml of resin was injected through a 3 mm cannula into the trachea. To cast the vascular system of the dog, about 300 ml of resin was injected into the pulmonary artery. The airway and vascular systems were not rinsed before casting. The dog lung was not fixed.

The lungs were placed in water at room temperature for three weeks. They were then placed in 5% HCl for 1 to 2 days, then rinsed in distilled water for two hours. Small specimens were taken from the lower lobe, mounted on aluminum stubs and sputter-coated with gold for three minutes at 0.1 torr (Ion coater, IB-5, Eiko Engineering Co., Mito City, Japan). They were observed with an ABT SX-40A scanning electron microscope (Akashi Beam Technology, Tokyo) operated at accelerating voltages ranging from 5 to 25 kV. The working distance ranged from 8 mm to 65 mm and micrographs were taken at 10X to 1,000X.

The diameter and the length of the terminal bronchioles and the respiratory bronchioles of the human airway casts and the diameter of the casts of the pulmonary arteries, alveolar capillaries, and holes in the alveolar capillary rings of the dog vascular casts were measured using a digitizer (IMS-Uniscience, Fukuoka City, Japan).

Diameter of capillaries and the diameter of the holes of alveolar capillary rings of the dog and human were compared with those published for the normal rat (Guntheroth *et al.*, 1982; Schraufnagel *et al.*, 1986). Student's-*t*-test was used as statistical method.

Results

By using the styrene resin and the described syringe, I was able to cast the lungs of large animals and fill all segments easily and economically (Figure 1). Furthermore, this method needs no lavage. It can be used both for macroscopic and scanning electron microscopic demonstrations. The cost of other commercially available resins is higher, when organs of large animals are desired to be cast.

Moreover, this method enabled me to measure many parts of the casts with a digitizer. In the present study, I show a terminal bronchiole of the lower lobe of the left human lung, and the pulmonary artery along the terminal bronchiole of the lower lobe of the left lung in the dog. The micrographs of the human specimen show that respiratory bronchioles, 500 μm in diameter, come off a terminal bronchiole that is about 1250 μm in diameter, by dichotomous branching (Figures 2 and 3a). The respiratory bronchioles led to short alveolar ducts. Alveolar ducts had almost the same widths as the respiratory bronchioles.

The alveoli of the human, at the end of the alveolar duct, varied in size. Many pits, fine particles, and fibers were observed on the uneven surfaces of the respiratory bronchioles and alveoli (Figures 2, and 3a-3c). Some epithelial cell-like structures (flat and cuboidal epithelial cells), and fibrous material were present on the surfaces of the respiratory bronchioles and the alveoli (Figure 3b).

The pulmonary arteries accompanied bronchioles (Figures 4-6 and 7-12). Oval and oblong nuclear impressions of endothelial cells (Kendall and Eissmann, 1980; Ohtani, 1980; Schraufnagel and Patel, 1990) were

Figure 1. A brass screw syringe (314 ml in volume) is shown.

Figure 2. Micrograph of a cast terminal bronchiole (1250 μm in diameter) with respiratory bronchioles (500 μm in diameter) and groups of alveoli in the human lung. Arrows show groups of alveoli; one group is shown enlarged in Figures 3a, 3b and 3c. Note tissue-like components on the surface of the terminal bronchioles. Bar = 1000 μm.

Figure 3a. A group of alveoli (at large arrow in Figure 2). Fine pits, and large and small fibers on the surfaces of the bronchioles, on the alveolar duct and on the alveoli are shown. The terminal airspace diameter ranges from 150 to 575 μm. Bar = 200 μm. **Figure 3b.** Higher magnification of the central part of alveoli in Figure 3a. Note a few pores (two arrowheads), small particles, a fiber and respiratory epithelial cell-like forms, and the epithelial cell I (flat, two large arrows) and II (cuboidal, small arrows) on the surfaces of alveoli. These two types of epithelial cells were distinguished by their form. Bar = 10 μm. **Figure 3c.** Higher magnification of the respiratory bronchioles, a short alveolar duct, and alveoli (at small arrow in Figure 2). Note many pits on their surface. Bar = 50 μm.

Figure 4. The cast of a bifurcated pulmonary artery (A) accompanied by a bifurcated bronchiole (T), prepared from a peripheral part of the left lower lobe of the dog. The region in the small square was filled with the resin as shown in Figure 7. Dorsal view of the cast lung. Bar = 1000 μm.

Figure 5. Higher magnification of a 500 μm large pulmonary artery (A) with an accompanying bronchiole (T) shown in the square in Figure 4. Note the circular indentations. Bar = 100 μm.

Figure 6. Higher magnification of the pulmonary artery in the square in Figure 5. Note many impressions coincided with the nuclei of endothelial cells of the pulmonary artery. Bar = 20 μm.

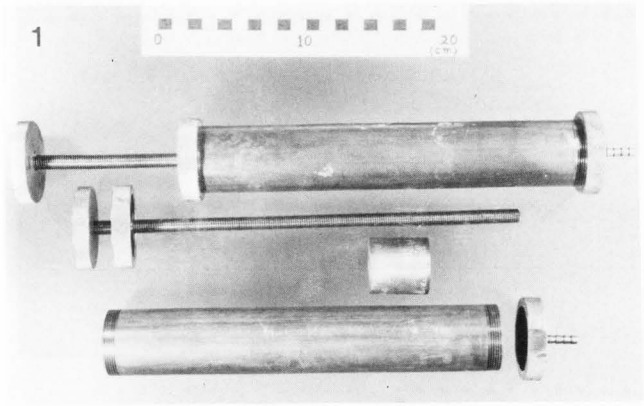
1
0
10
20
(cm)

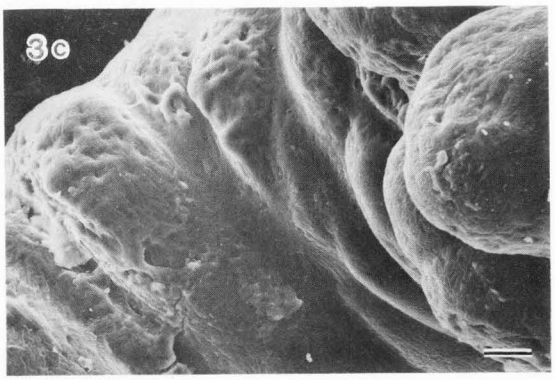
3c

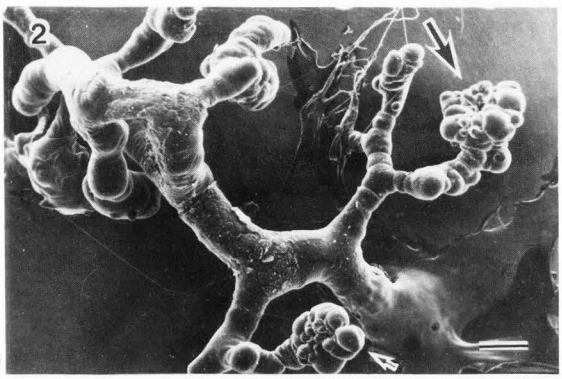
2

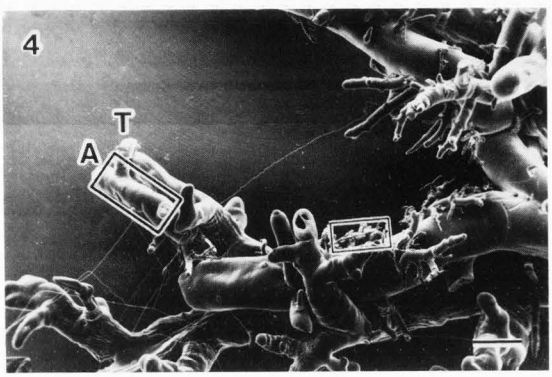
4
T
A

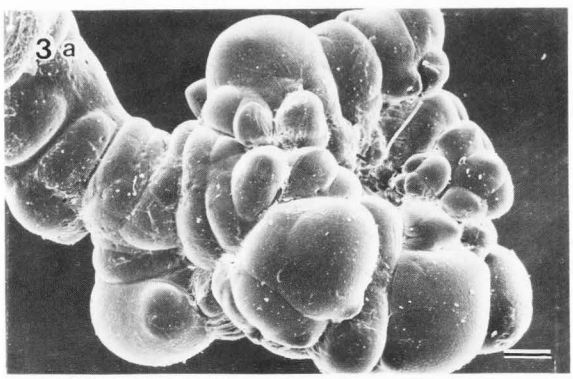
3a

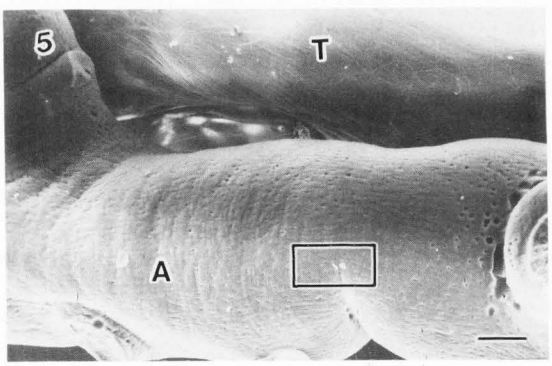
5
T
A

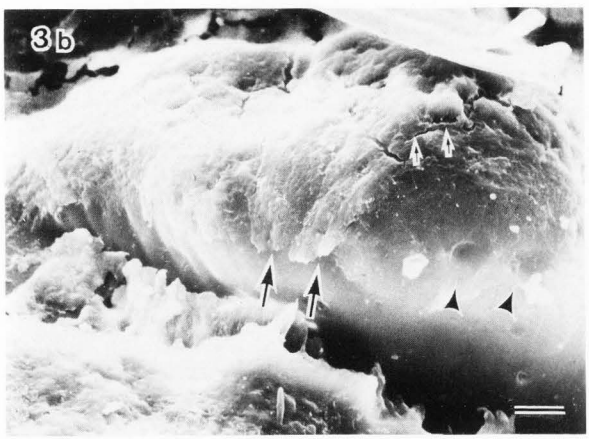
3b

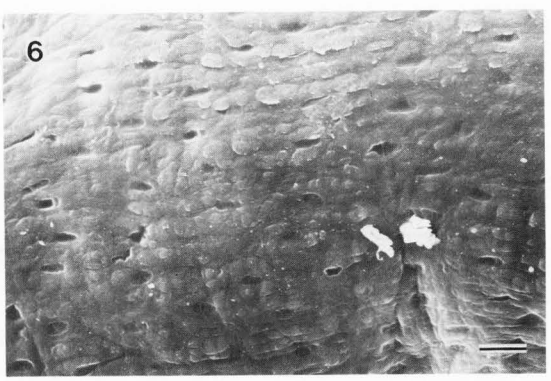
6

Table 1. Diameter of alveolar capillaries and alveolar capillary interspaces in the normal dog and rat.

	Alveolar capillaries			Alveolar capillary interspaces (holes)		
	n	m (μm)	SD	n	m (μm)	SD
Dog[1]	22	6.35	2.29	30	5.73	1.27
Rat[2]	100	6.75	1.4	26	4.23	1.2
Rat[3]	26	5.78	1.17*			

m = mean diameter; [1]this paper, Figure 12; [2]Schraufnagel *et al.*, 1986; [3]Guntheroth *et al.*, 1982
*The standard deviation (SD) was calculated from the standard error.

observed on the surface of the cast pulmonary arteries (30 to 500 μm in diameter; Figures 5-8). Round impressions were found on capillaries that were about 12 μm in diameter (Figure 10); these are also regarded as caused by the nuclei of endothelial cells (Kendall and Eissmann, 1980). On the cast arteries (Figures 4-6), there were circular indentations.

The capillary networks in the dog had two distinct patterns. The loose network (Figures 8 and 9) that appeared on the pleural surface and around the arteries and airways and the denser network that was around alveoli (Figures 10-13).

In the dog, the pulmonary arteries (Figure 8) were about 40 μm wide when viewed dorsally (Figures 7 and 8). They gave off 6 single branches along their course. The diameter of these branches varied between 10 to 20 μm (Figures 7 and 8). The alveolar capillaries were concave (basket-like) and were closely apposed, forming groups when viewed ventrally (Figures 11-13). There were three kinds of holes of the capillaries in the dog, large (Figures 8 and 9), small (Figures 11-13) and slit-like (Figure 10).

The diameter of capillaries and the holes of alveolar capillary rings in the dog and human obtained from a micrograph (Figure 12) in the present study were compared to those published for the normal rat (Guntheroth *et al.*, 1982; Schraufnagel *et al.*, 1986). The diameter of capillaries in the dog lung and rat lung was similar but the diameter of the holes of alveolar capillary rings in the dog was larger than that in the normal rat ($p < 0.001$; Table 1). Likewise, the diameter of the capillaries on the ventral and dorsal surfaces were similar (Table 2).

Discussion and Conclusion

I have made human and other mammalian lung casts using styrene-methylethylketone resin with the screw syringe and a rubber tube for macroscopic demonstration. This study shows that these casts can withstand the electron beam in the scanning electron microscope and the obtained views are of good quality allowing them to be compared to the views of other authors. When large amounts of resin are required, this method is recommended because it is economical and produces casts of good quality.

A screw syringe was used for small sized animals (e.g., the toad; Lametschwandtner *et al.*, 1976; 1990). The screw syringe with the rubber tube for constant pressure, as used for various sized animals (e.g., humans and dogs, the present study; other studies, Hojo, 1974; 1975a; 1975b; 1980; Hojo *et al.*, 1989) is also

Figure 7. Low magnification micrograph of pulmonary arteries and capillaries. Dorsal view in the lung cast of the dog. Bar = 50 μm.

Figure 8. Higher magnification of an area pointed by a large arrow in Figure 7. Note endothelial cell nuclei impressions pointed by two large arrows on the pulmonary artery (40 μm). A right-angled branch (pointed by the upper asterisk) led to the loose capillary network. The lower asterisk marks another branch of the artery. Note large holes of the capillary network. Bar = 20 μm.

Figure 9. Higher magnification of the loose capillary network shown in Figure 8. Note the larger capillary holes. Bar = 10 μm.

Figure 10. Higher magnification of the square in Figure 7. Note the constriction of the connection site of capillaries (small arrows) and round-shaped nucleic impressions (two large arrows) on the capillary. Note a few slit-like holes distinct from holes in Figures 8, 9, 11, 12 and 13. The length of the slit-like hole in the central area (the largest arrow) is 14 μm. The long axis of the central slit-like hole is in parallel with plane of this micrograph. Bar = 10 μm.

Figure 11. Higher magnification of the central area of the ventral view in Figure 8. Note basket-like structures shown in the angled area. Bar = 25 μm.

Figure 12. Higher magnification of the angled area in Figure 11. Note small holes of the capillary network. These holes were smaller than those shown in Figures 8 and 9. Bar = 12.5 μm.

Figure 13. Higher magnification of the capillary network in the angled area in Figure 12. Bar = 5 μm.

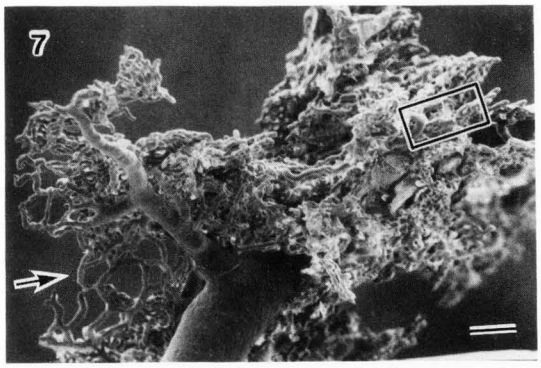

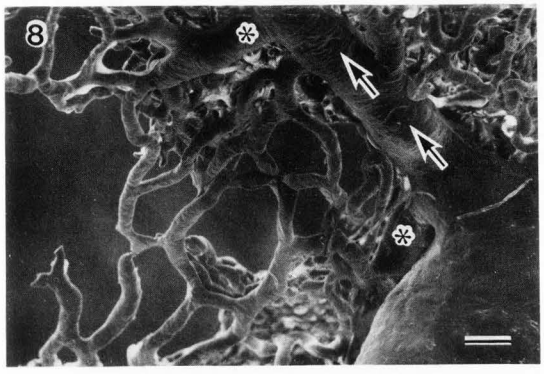

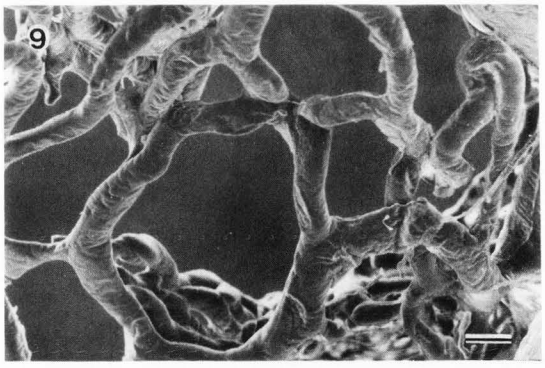

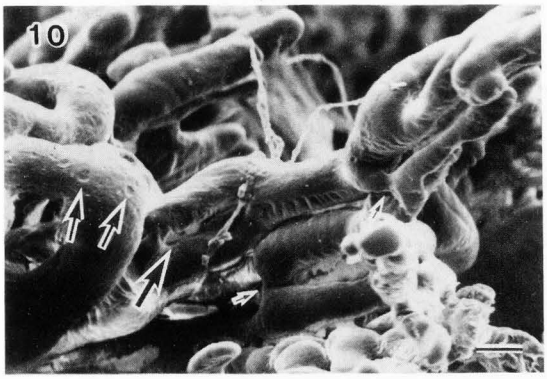

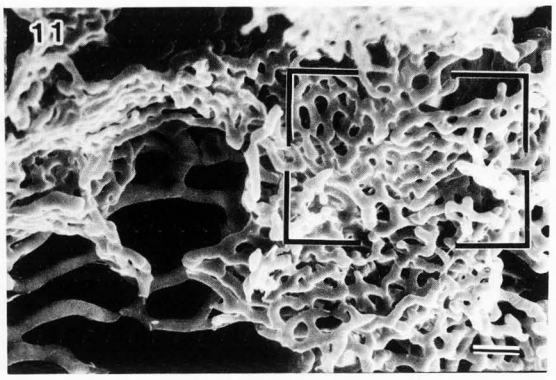

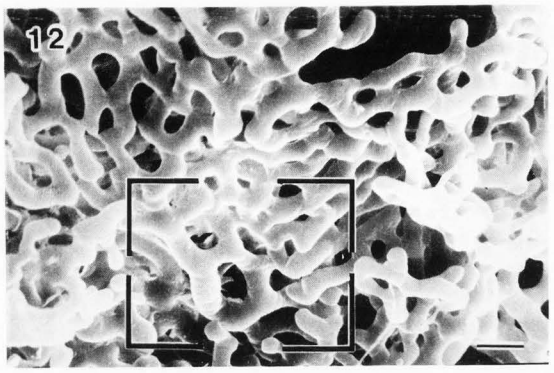

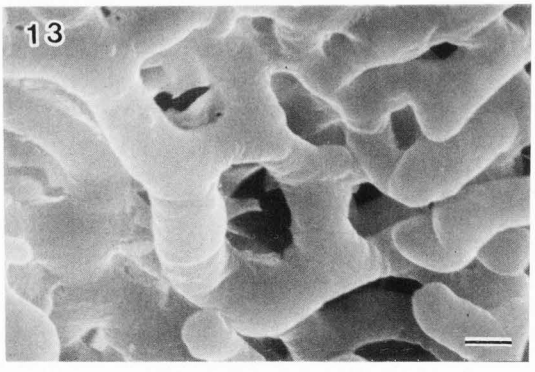

Table 2. Difference of the capillary diameters between the dorsal and the ventral view.

	n	m (μm)	SD
Dorsal view (Figure 10)	12	6.05	2.08
Dorsal view without constricted connecting capillaries (Figure 10)	9	7.70	1.18
Ventral view (Figure 13)	16	6.01	1.12

useful for the examination with the scanning electron microscope. For applying this method, the best injection pressure is 44 mm Hg for the airways, which is greater than the pressure used by Dilly (1986) and Wang (1990), and 110 mm Hg for the vascular injection, which is similar to that used by Hossler and West (1988). The screw syringe and the rubber tube in this method are suitable for keeping the injection pressure almost constant resulting in good casts. Among a group of the alveoli, central ones were about 150 to 200 μm in diameter, but peripheral ones were about 575 μm in diameter (Figure 3a). These data were similar to those of the adult subjects obtained by Dilly (1986), but in the Dilly's study, the injection pressure for the airway was 30 cm H_2O (= 22 mm Hg).

The pits in the cast represent protuberances from cells of the respiratory bronchioles and the alveoli (Figures 3a-c) or fibrous materials in the respiratory bronchioles and the alveoli of the human lung (Figures 2, 3a and 3b). Some of the pores of the alveoli were regarded as alveolar pores which Wang (1990) described on the surfaces of adult human alveoli. These pores or pits observed on alveoli were also reported by other authors (Schraufnagel, 1990). In the present study the impressions of the endothelial cell nuclei were observed on capillaries with a luminal diameter of 12 μm (Figure 10). Similar impressions have been observed on the surface of veins of about 200 μm diameter by Hossler and West (1988). Fibrous materials in the respiratory bronchioles and the alveoli may be those inspired when this subject worked in a factory.

The loose and the dense capillary networks have been described by other authors (Guntheroth *et al.*, 1982; Schraufnagel *et al.*, 1986). Measurements of capillaries of these two networks were compared. The mean diameter of the alveolar capillaries by Schraufnagel *et al.* (1986) was 6.75 μm and that by Guntheroth *et al.* (1982) was 5.78 μm (Table 1). The difference in the average diameters of alveolar capillaries between these two studies was significant ($t = 2.1698$, $p < 0.05$); but the difference in the average diameter of alveolar capillaries evaluated by Guntheroth *et al.* (1982) and that estimated in the present study, was not significant. The average diameter of holes of the alveolar capillary rings in the dog (present study) was significantly larger than that of the rat in the study of Schraufnagel *et al.* (1986; $t = 4.521$, $p < 0.001$). This is one of the differences in the lungs between the dog and the rat.

Some distinct circular indentations were observed on the surface of the cast arteries in the dog lung. These indentations may be caused by the smooth muscle of the arterial wall and may be involved in blood flow regulation in the pulmonary arteries. The same function has been suggested for pulmonary veins by Aharinejad *et al.* (1991a; 1992) and Schraufnagel (1990).

This method does not require lavage of blood vessels and airways as do other methods (e.g., Lametschwandtner *et al.*, 1990; Schraufnagel, 1990; Schraufnagel and Schmid, 1988). By omitting rinsing of blood vessels and airways, inhaled materials and tissue remnants can be preserved and observed. Moreover, as pits on the inner walls of the respiratory bronchioles and alveoli, and fine round impressions on the inner walls of 12 μm capillaries were observed, I conclude that the suggested casting material fills airways and the arterial system without shrinkage, and that these casts may be useful in further steps of scanning electron microscopic three-dimensional analyses and in computer-assisted measurements of bronchioles, pulmonary arteries, capillaries, alveoli, tissue remnants and inhaled materials in the lung of humans and other mammals. In addition, macroscopic anatomic studies of the cast lung specimens (without preceding lavage of blood vessels and airways) can be performed.

References

Aharinejad S, Böck P, Lametschwandtner A, Franz P, Firbas W. (1991a). Spincters in the rat pulmonary veins. Comparison of scanning and transmission electron microscopic studies. Scanning Microsc. **5**: 1091-1096.

Aharinejad S, Lametschwandtner A, Böck P, Franz P. (1991b). Microvascularization of the pleura in rats and guinea pigs. Scanning Microsc. **5**: 1097-1103.

Aharinejad S, Böck P, Lametschwandtner A, Firbas W. (1992). Scanning and transmission electron microscopy of venous sphincters in the rat lung. Anat. Rec. **233**: 555-568.

Charan NB, Turk GM, Dhand R. (1984). Gross and subgross anatomy of bronchial circulation in sheep. J. Appl. Physiol. **7**: 658-664.

Dilly SA. (1986). Microcorrosion casting of the human respiratory acinus. Scanning Electron Microsc. **1986**;III: 1095-1101.

Guntheroth WG, Luchtel DL, Kawabori I. (1982). Pulmonary microcirculation: tubules rather than sheet and post. J. Appl. Physiol. **3**: 510-515.

Hodde KC, Steeber DA, Albrecht RM. (1990). Advances in corrosion casting methods. Scanning Microsc. **4**: 693-704.

Hojo T. (1974). A reexamination on making anatomical corrosion casts, especially from the lung. Sapporo Med. J. **43**: 1-4 (in Japanese).

Hojo T. (1975a). On trachea, bronchi and pulmonary vessels of the harbor seal with a corrosion cast. In: Proc. of 10th Int. Cong. Anat. Yamada E (ed.), Science Council of Japan, Tokyo, Japan, p. 86 (abstract).

Hojo T. (1975b). An anatomical study on trachea, bronchi and pulmonary vessels of the harbor seal (*Phoca vitulina*) with a corrosion cast. Acta Anat. Nippon **50**: 229-235.

Hojo T. (1980). Corrosion anatomy of the eparterial bronchi in the rough toothed porpoise, *Steno bredanensis*. J. Univ. Occup. Environ. Health **2**: 463-468.

Hojo T, Nakashima T, Hayashi H, Hijioka A. (1989). The tracheobronchial tree and the pulmonary

vascular pattern of the rough toothed porpoise, *Steno bredanensis*. Acta Anat. Nippon. **64**: 108 (abstract; in Japanese).

Hossler FE, West RF. (1988). Venous anatomy and morphometry: Studies on the duckling using vascular corrosion casting. Am. J. Anat. **181**: 425-432.

Kendall M, Eissmann E. (1980). Scanning electron microscopic examination of the human pulmonary capillaries using a latex replication method. Anat. Rec. **196**: 275-283.

Koike K, Ohnuki T, Ohkuda K, Nitta S, Nakada T. (1986). Branching architectures of canine pulmonary arteries: A quantitative cast study. Tohoku J. Exp. Med. **149**: 293-305.

Lametschwandtner A, Simonsberger P, Adam H. (1976). Scanning electron microscopical studies of corrosion casts. The vascularization of the preventricular organ (organum vasculosum hypothalami) of the toad, *Bufo bufo* L. Mikroskopie **32**: 195-203.

Lametschwandtner A, Lametschwandtner U, Weiger T. (1990). Scanning electron microscopy of vascular corrosion casts - technique and applications: Updated review. Scanning Microsc. **4**: 889-941.

Ohtani O. (1980). Microvasculature of the rat lung as revealed by scanning electron microscopy of corrosion casts. Scanning Electron Microsc. **1980**; III: 349-356.

Piasecki C. (1974). A simple method to produce high quality corrosion casts. Med. Biol. Illus. **24**: 86-90.

Rodriguez M, Bur S, Favre A, Weibel ER. (1987) Pulmonary acinus: Geometry and morphometry of the peripheral airway system in rat and rabbit. Am. J. Anat. **180**: 143-155.

Schlesinger RB, McFadden LA. (1981). Comparative morphometry of the upper bronchial tree in six mammalian species. Anat. Rec. **199**: 99-108.

Schraufnagel DE. (1987). Microvascular corrosion casting of the lung. A state-of-the-art review. Scanning Microsc. **1**: 1733-1747.

Schraufnagel DE. (1990). Corrosion casting of the lung for scanning electron microscopy. In: Electron microscopy of the lung. Schraufnagel DE (ed.); Lung Biology in Health and Disease. Vol. 48. Lebfant C. (Executive Editor). Marcel Dekker, New York, pp. 257-297.

Schraufnagel DE, Mehta D, Harshbarger R, Treviranus K, Wang NS. (1986). Capillary remodeling in Bleomycin-induced pulmonary fibrosis. Am. J. Pathol. **125**: 97-106.

Schraufnagel DE, Patel KR. (1990). Sphincters in pulmonary veins: An anatomic study in rats. Am. Rev. Respir. Dis. **141**: 721-726.

Schraufnagel DE, Schmid A. (1988). Microvascular casting of the lung: Vascular lavage. Scanning Microsc. **2**: 1017-1020.

Wang NS. (1990). Scanning electron microscopy. In: Electron microscopy of the lung. Schraufnagel DE (ed.); Lung Biology in Health and Disease. Vol. 48. Lebfant C. (Executive Editor). Marcel Dekker, New York, pp. 517-555.

Discussion with Reviewers

S. Aharinejad: Why did you use an acceleration voltage of 25 kV? Is it not too high?
Author: I correlated the acceleration voltage to the surface feature of the specimens. In this study, the voltage of 5 kV was used for the capillary network of the dog lung.

S. Aharinejad: What volume of your resin was used for individual specimens?
Author: As stated in the text, about 700, 500 and 300 ml of resin were used for the human trachea, dog trachea, and human arterial system, respectively.

A. Lametschwandtner: There are tissue remnants adhering to the cast surface. Is this due to insufficient maceration or to plastification of tissue components by the resin mixture used?
Author: As lungs were not rinsed before casting, and as lungs were fixed with formalin, plastification of tissue remnants was observed in Figures 2, 3a and 3b.

S. Aharinejad: You have got very good views of the pulmonary artery in dogs. Did you observe any venous vessels in the canine pulmonary microvascular bed? Have you ever observed any constrictions on venous vessels, suggesting the presence of venous sphincters?

Figures 4 and 5 show the canine pulmonary arteries. On the surface of these cast arteries, some circular indentations can be distinguished, some of them are very impressive. Would you think of a probable occurrence of arterial sphincters in the dog lung? What functional implications would you expect?
Author: I have not examined the constrictions of the pulmonary veins. On the surface of the pulmonary arteries in the dog, I also observed many distinct circular indentations (Figures 4 and 5). I think that these circular narrowing may be caused by smooth-muscle contraction as described previously on the wall of the pulmonary veins (Aharinejad, *et al.*, 1991a; 1992; Schraufnagel, 1990). The smooth-muscles of the arterial wall described are suggested to be related with the blood flow regulation.

K. Hodde: When in time does the viscosity of the ready injection medium change to higher values, and when is setting complete? How meaningful statistically is it to compare the measurements in one specimen with those in the literature gathered with different methods and materials?
Author: The resin used easily sets by evaporation of the methylethylketone in a week, but in about 3 weeks for the lung. The comparisons of the data of this study with those of other studies showed almost equal values in the human terminal airspaces, but showed differences in the dog pulmonary arteries, which may be related with their various body sizes.